A Comparison of Net and Continuum Theory as Applied to Cord-Reinforced Laminates

Samuel K. Clark and Richard N. Dodge

Department of Engineering Mechanics, University of Michigan, Ann Arbor, Michigan 48104, U.S.A.

Abstract

The basic formulation of plane stress-analysis techniques for textiles imbedded in rubber is given both from the viewpoint of a load-carrying net and of a continuous elastic material with orthotropic properties. The developments are basically dissimilar, and yet it is shown that, for material properties commonly encountered in rubber-coated textiles, both theories predict essentially the same textile loads, although the stresses carried by the rubber matrix differ in the two theories. This shows that the network approach, which is by far the simpler of the two, is perfectly valid for purposes of estimating cord load in cord-rubber structural members.

A method is presented through the use of either theory to compute the fraction of load carried by the cord network and the fraction carried by the rubber matrix.

Introduction

At least two techniques are in common use for the evaluation of cord loads in rubber-impregnated cord structures, such as commonly used in pneumatic tires and other rubberized structural members. One point of view focuses on the network of textile cords, due to the fact that their elastic stiffness is so much greater than the rubber in which they are imbedded. The usual procedure is to completely neglect the presence of the rubber and to deal with the loads carried by the net alone. This process is straightforward but requires large and nearly unrestrained deformations of the net in order to accommodate biaxial stress states whose normal force resultants do not lie parallel to the cord network. This type of analysis is most common in two-dimensional or plane structures where the net may be treated as a two-dimensional set of lines and the membrane stress is determined accordingly. Little effort has been made to adapt such net formulations to bending-stress problems.

A second possible technique for conducting a stress analysis of a regular array of cords imbedded in some softer material is to consider the entire structure as an elastic continuum with the proper orthotropic elastic properties. In the case of twisted cords, such as commonly used in pneumatic tires, it is necessary to imagine that the cords are untwisted and the filaments uniformly dispersed throughout the matirx, so that the orthotropic elastic properties become continuous across the width and thickness of the body in question. This avoids the mathematical difficulties of concentrated anistropy which is, of course, the true description of the material, and yet provides a reasonably accurate overall or gross picture of the deformation characteristics of the body in question. Such an approach neglects the local effects of the cords, but it does accurately represent phenomena averaged over at least several cord diameters and spaces. This type of analysis has been pursued by a number of authors interested both in applications of cord-reinforced rubber and in applications of fiber- and filament-reinforced materials of higher strength. Such materials have been studied in the plane case by Akasaka [1], by Azzi and Tsai [2], and by Clark [3], while a complete theory has been given by Resissner and Stavsky [6]. A thorough discussion of the elastic properties and stress-analysis techniques associated with this continuum approach to materials has recently been given by Hofferberth and Frank [5]. While some effort has been devoted to the study of bending characteristics in such materials, primarily by Reissner and Stavsky, most of the published information concerns membrane effects. Whitney [8] has recently pointed out that plane, symmetric materials commonly studied in the cited references are sym-

metric only insofar as their membrane characteristics are concerned. They are completely unsymmetric in regard to bending.

With the complete theory of Reissner and Stavsky available, it seems most probable that the bending characteristics of such fiber-reinforced materials will be approached from the continuum point of view, and that such analysis only requires determination of the proper elastic constants for its complete implementation. On the other hand, plane or membrane stress problems may apparently be done by either method, and there are significant advantages to the net analysis approach in membrane stress analysis since it represents a far simpler technique in most cases. Further, the results may be more easily interpreted in terms of their physical effects on the composite cord-rubber structure. This is particularly true when the cords or reinforcing elements are significantly stiffer than the matrix in which they are imbedded. This is commonly the case in pneumatic-tire construction, as well as in many other applications of rubber-coated fabrics, but not necessarily so true in regard to fiber-reinforced plastics or whisker-reinforced metals.

Net Analysis

Here, a symmetric multi-ply laminate is treated as an inextensible plane net of cords imbedded in a softer matrix. The cords in successive plies form positive and negative angles with an axis of symmetry, such as shown in Figure 1. A portion of the total load applied to the laminate is carried by the net and the remainder by the matrix. These different portions are found by evaluating the load-carrying capability of the net and by requiring that any remaining load be carried by the softer matrix. The load carried by the net causes net deformation caused by the change in cord angle, and, since the matrix is attached to the net, it must also deform in a similar manner. Utilizing equilibrium conditions and deformation compatibility requirements, the loads carried by the net and the matrix can be found, as can the resulting deformations.

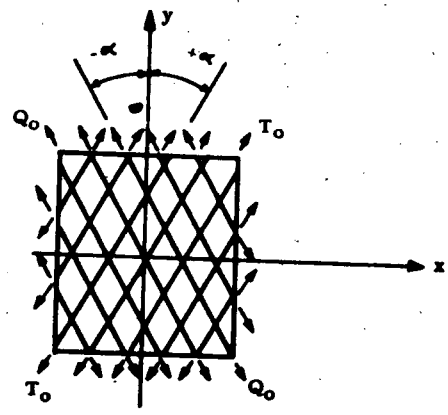

Fig. 1. Loaded element of net.

Fig. 1. Loaded element of net.

In carrying out this net analysis, one begins by assuming cord loads in the net. These net loads are then resolved into the principal directions or directions of symmetry of the original laminate so that the total external imposed stress may be expressed as a function of these cord loads. The element used for this analysis is illustrated in Figure 1, where T_0 and Q_0 are the loads per cord in alternate plies. Loads in alternate plies are assumed to be different until otherwise determined, i.e., both T_0 and Q_0 are independent unknowns. However, it is assumed that each set of cords running in the same direction carries the same load per cord. We assume an even number of plies to maintain approximate membrane symmetry and orthotropy, along with the assumption that the thickness is small enough, compared to the other dimensions, so that this may be considered a plane structure with vanishing or unimportant thickness effects. In addition, it will be convenient to let each ply have the same physical and geometric characteristics, except for the cord angle, although this requirement can be avoided where desirable.

In Figure 1, x and y represent the principal directions of elasticity while α is the angle made by the cords with the y axis. By letting n_c be the number of cords per unit length measured perpendicular to the cord direction and n_p the total number of plies, then the normal force per unit length on the y face is

$$N = \tfrac{1}{2}(T_0 + Q_0) \cdot n_c \cdot n_p \cdot \cos^2\alpha \qquad (1)$$

Similarly, the normal force per unit length on the x face is

$$N_x = \tfrac{1}{2}(T_0 + Q_0) n_c \cdot n_p \sin^2\alpha = N \cdot \tan^2\alpha \qquad (2)$$

The shear force per unit length on each face is

$$S = \tfrac{1}{2}(T_0 - Q_0) n_c \cdot n_p \sin\alpha \cos\alpha \qquad (3)$$

T_0 and Q_0 are independent variables, i.e., may be specified arbitrarily. Using Equations 1, 2, and 3, the independent variables may now be considered as N and S. Physically, this means that any magni-

tude of shear force S will be carried completely by the symmetric net arrangement, since S may be specified arbitratily. However, only one ratio of normal forces in the x and y direction may be carried by the net alone, since $N_x = N \tan^2\alpha$ at all times. Thus, a net may be thought of as an array which, when viewed from principal axes laid out along the bisectors of the cord angles, carries any shear without deformation and any set of normal membrane forces in the ratio $N_x = N \tan^2\alpha$. The net array only deforms under those normal forces which are not in the ratio $N_x = N \tan^2\alpha$, and, hence, the role of the matrix in which the net is imbedded is to carry such "excess" normal membrane forces. The load distribution carried by the net is illustrated in Figure 2.

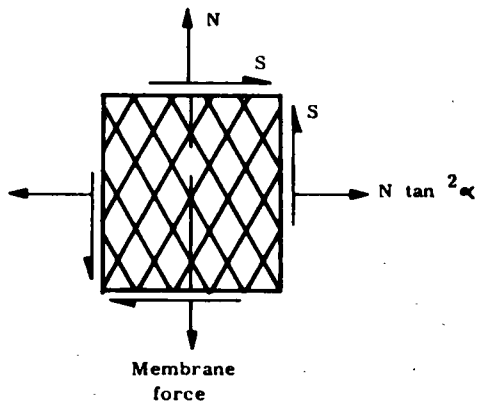

Fig. 2. Membrane-force distribution under cord loads.

Under a general stress state, a portion of the total load is carried by the net and a portion carried by the matrix. The net loads are shown in Figure 2. Figure 3 is a sequence of sketches illustrating the net and matrix both before and after application of some general load. In Figure 3, S_y, S_x, and S_{xy} are the applied general stresses, while t_y and t_x are the stresses carried by the matrix. This implies, of course, that all of the applied shear stress is carried by the net, as previously discussed.

The net deforms under load, resulting in a new cord angle. The matrix deforms accordingly. This means the unknowns N, α', t_y, and t_x must be found in terms of the applied stresses and the original cord angle α. The equations available for this are those of equilibrium and of strain or deformation compatibility. The equilibrium equations are

$$N + t_y \cdot n_p \cdot H = S_y \cdot n_p \cdot h \tag{4}$$

$$N \cdot \tan^2\alpha' + t_x \cdot n_p \cdot H = S_x \cdot n_p \cdot h \tag{5}$$

where h is the thickness of an individual ply, d_c is the cord diameter and

$$H = \left(h - \frac{\pi}{4} d_c^2 \cdot n_c\right)$$

H is the effective area of the matrix per unit length for each individual ply.

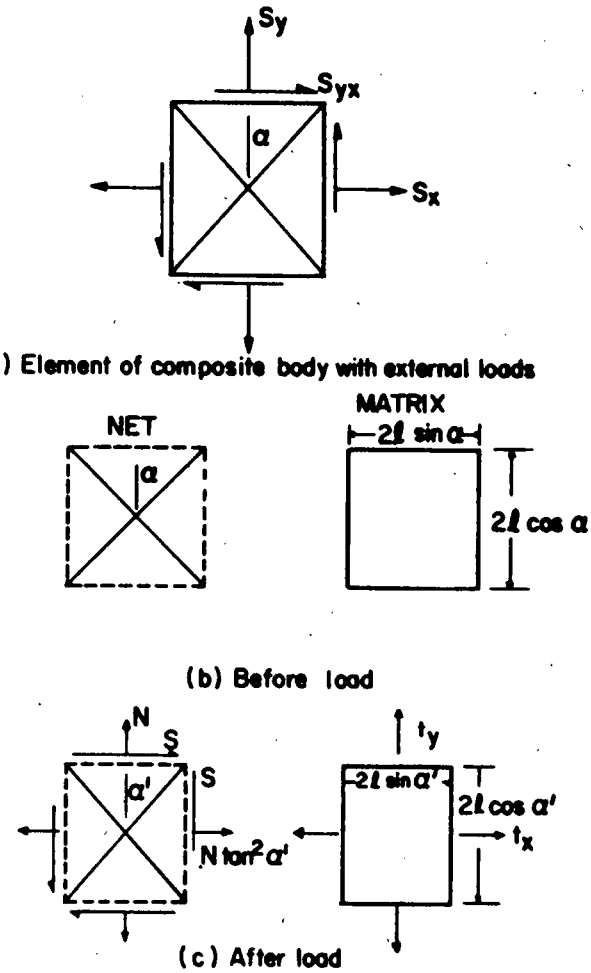

Fig. 3. Element of laminate before and after applied load.

Strain compatibility arises from the fact that the deformation of the matrix in the x and y directions must correspond to that of the net in those directions. For small strains, conditions are represented by the equations

$$t_y = E[(\cos\alpha'/\cos\alpha - 1) + \mu(\sin\alpha'/\sin\alpha - 1)]/(1 - \mu^2) \tag{6}$$

$$t_x = E[(\sin\alpha'/\sin\alpha - 1) + \mu(\cos\alpha'/\cos\alpha - 1)]/(1 - \mu^2) \tag{7}$$

where E and μ are the Young's modulus and Poisson's ratio of the matrix for small strains. It

should be noted that Equations (6) and 7 are constructed here on the basis of infinitesimal strain or deformation, sincd this is the simplest and most readily recognizable stress–strain law. It will be shown below that equations similar to 6 and 7 can be written for finite deformations. Equations 4 and 5 are valid independent of the magnitude of the deformation, since the stresses t_x, t_y, S_x, and S_y are referred to the original area. Since all of the applied shear stress is carried by the net, shear stress does not enter into the matrix stress-strain relations and the matrix is free of shear deformation.

Substituting t_y and t_x Equations 6 and 7 into Equations 4 and 5 gives

$$S_y = N/(h_p \cdot h) + \frac{E \cdot H}{h(1-\mu^2)}\left[(\cos\alpha'/\cos\alpha - 1) + \mu(\sin\alpha'/\sin\alpha - 1)\right] \quad (8)$$

$$S_x = N\tan^2\alpha'/(n_p \cdot h) + \frac{E \cdot H}{h(1-\mu^2)} \times \left[\sin\alpha'/\sin\alpha - 1) + \mu(\cos\alpha'/\cos\alpha - 1)\right] \quad (9)$$

H/h is the ratio of the total volume of a given element to the matrix volume in that same element. Eliminating N from Equations 8 and 9 results in the following transcendental equation for the final cord angle α' of the net

$$\{[(\sin\alpha'/\sin\alpha - 1) + \mu(\cos\alpha'/\cos\alpha - 1)] - \tan^2\alpha'[(\cos\alpha'/\cos\alpha - 1) + \mu(\sin\alpha'/\sin\alpha - 1)]\} = \frac{S_y \cdot h \cdot (1-\mu^2)}{E \cdot H}\left(\frac{S_x}{S_y} - \tan^2\alpha'\right) \quad (10)$$

It is instructive to write the right-hand side of Equation 10 in the dimensionless form indicated, since it shows that the final cord angle depends not only on the magnitude of the ratio of applied stresses to the matrix modulus, as given by the quantity

$$\frac{S_y \cdot h \cdot (1-\mu^2)}{E \cdot H}$$

in Equation 10, but also upon the ratio of the two applied stresses S_x/S_y. After some consideration of Equation 10, it may be demonstrated that for those cases where the ratio S_x/S_y on the right side is exactly equal to $\tan^2\alpha'$, then the solution to Equation 10 for the final angle α' of the net is exactly equal to the original angle α. In other words, the unique solution for a zero right-hand side of Equation 10 is $\alpha = \alpha'$. This means that a net loaded in such a way that the applied force vectors are colinear with the cord directions in this symmetric net results in no change of the geometry of the net. This is to be expected from physical considerations. For those cases where such a simple solution to Equation 10 does not exist, it is necessary to use it to determine the final angle α' of the network. In addition, one must also draw upon the fact that all of the applied shear loads are carried by the net itself so that the applied shear stresses are related to the quantity S through Equation 11

$$S = S_{yx} \cdot n_p \cdot h \quad (11)$$

The value of α' found from Equation 10 may be used in either Equation 8 or 9 to obtain N. The quantity S may be obtained from Equation 11, and these values can then be used in Equations 6 and 7 to obtain the stresses carried by the matrix. Equations 4 and 5 give the cord loads T_0 and Q_0 ,which may also be obtained from the direct solution for these cord loads in the form given by Equation 12

$$T_0 = \left[\frac{N}{n_p \cdot \cos\alpha} + \frac{S_{yx} \cdot h}{\sin\alpha}\right] \Big/ (n_c \cdot \cos\alpha)$$
$$Q_0 = \left[\frac{N}{n_p \cdot \cos\alpha} - \frac{S_{yx} \cdot h}{\sin\alpha}\right] \Big/ (n_c \cos\alpha) \quad (12)$$

The final angle obtained from Equation 10 depends on the linearity of the stress–strain relation as expressed in Equations 6 and 7. Generally, this is only good for relatively small ranges of strain, which means small ranges of cord-angle change. Even when the cords are inextensible, there can be large angle changes which result in finite deformations of the matrix. An additional refinement to this previous theory can be made by substituting a finite deformation stress–strain law in place of Equations 6 and 7. These new equations may be used with Equations 4 and 6 to form a general, finite deformation theory which is not subject to the indicated restrictions.

Referring to Figure 4 for notation, let the matrix stresses t_x, t_y, and t_s be referred to the original or unstrained area of the element. Let the ratios of final lengths to original lengths of the sides of the element be called extension ratios λ_x, λ_y, and λ_s. Then a good approximation to the stress–strain curve of rubber is shown by Treloar [7] to be given by the expressions

$$\lambda_x t_x - \lambda_z t_z = G(\lambda_x^2 - \lambda_z^2) \quad (13)$$

$$\lambda_z t_z - \lambda_y t_y = G(\lambda_z^2 - \lambda_y^2) \quad (14)$$

Using the condition of incompressibility in the form of

$$\lambda_x \lambda_y \lambda_z = 1 \quad (15)$$

and noting that $t_z = 0$ for the plane problem in question, then Equations 13 and 14 may be written as

$$t_x = G\left(\lambda_x - \frac{1}{\lambda_x^3 \lambda_y^2}\right) \quad (16)$$

$$t_y = G\left(\lambda_y - \frac{1}{\lambda_x^2 \lambda_y^3}\right) \quad (17)$$

A set of equations analogous to Equations 4–7 may now be written as follows

$$N + n_p \cdot t_y \cdot H = S_y \cdot n_p \cdot h \quad (18)$$

$$N \cdot \tan^2\alpha' + n_p \cdot t_x \cdot H = S_x \cdot n_p \cdot h \quad (19)$$

$$t_x = G\left(\lambda_x - \frac{1}{\lambda_x^2 \lambda_y^2}\right) \quad (20)$$

$$t_y = G\left(\lambda_y - \frac{1}{\lambda_x^2 \lambda_y^3}\right) \quad (21)$$

$$\lambda_x = \frac{\sin\alpha'}{\sin\alpha} \quad (22)$$

$$\lambda_y = \frac{\cos\alpha'}{\cos\alpha} \quad (23)$$

Equations 18–23 may be combined in a fashion similar to Equations 4–7. The result of eliminating all unknown cord loads and matrix stresses is again a characteristic equation relating the final cord angle of the symmetric net to the initial cord angle. This takes the form of

$$\left\{\left(\frac{\sin\alpha'}{\sin\alpha} - \frac{\sin^3\alpha \cos^2\alpha}{\sin^3\alpha' \cos^2\alpha'}\right) - \tan^2\alpha'\left(\frac{\cos\alpha'}{\cos\alpha} - \frac{\sin^2\alpha \cos^3\alpha}{\sin^2\alpha' \cos^3\alpha'}\right) = \frac{S_y \cdot h}{GH}\left(\frac{S_x}{S_y} - \tan^2\alpha'\right)\right\} \quad (24)$$

Equation 24 is the characteristic equation governing the deformation of the cord-matrix combination. In general, after solution of Equation 24 for the final, deformed cord angle α', one may return to Equations 22 and 23 in order to determine the extension ratios, and from there to Equations 20 and 21 to determine the matrix stresses. These then allow determination of cord loads by means of Equations 18 and 19. It should be noted that all shear stresses are still presumed to be taken by the cord network, so that Equations 11 and 12 are still valid. This allows all internal characteristics of the network to be determined in terms of the final geometry.

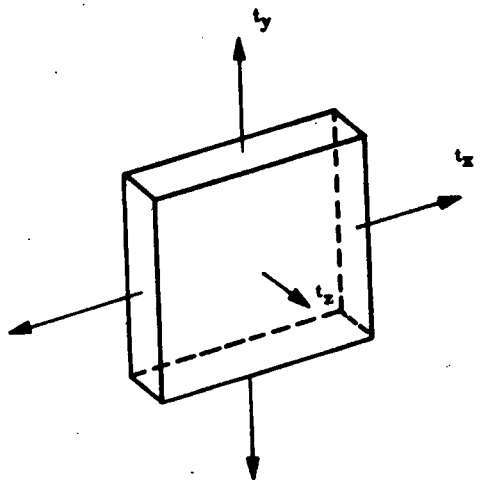

Fig. 4. Principal stresses in the matrix.

Equation 24 also illustrates the fact that the final deformed shape of the net is dependent upon the shear modulus of the matrix material, so that in the limiting case, as the shear modulus increases indefinitely, the cord angle remains unchanged during loading. It may be demonstrated that a zero right-hand side of Equation 24 results in a unique solution to it, in which the angle α' is identical to the original angle α. This means that no net deformation will be present for all cases where the ratio of applied stresses S_x/S_y is equal to $\tan^2\alpha'$. Under such conditions, the initial and final cord angles will be identical. For other cases, where the right-hand side does not vanish, it is seen that the net deformation is proportional to the magnitude of the applied stress S_y, as well as inversely proportional to the shear modulus G, as previously discussed.

Let the change in angle be small, so that for a particular case,

$$\alpha' = \alpha + \delta$$

where δ is much smaller than α or α'. Then it may be shown that under this condition both Equations 10 and 24 reduce to an identical form. This is to be expected, and serves as one check on their validity. In general, the more exact Equation 24 would be

preferred as a means of calculating the final net angle α', since both Equations 10 and 24 are complex enough so that solutions can only be obtained by numerical trial and error methods.

Continuum Analysis

A thin, multi-ply cord-rubber laminate is treated as a plane orthotropic elastic continuum. In this analysis, a general plane-stress state applied in the principal directions of elasticity is transformed to the directions of the cords and orthogonal to them. If one assumes that the strain in the cord direction vanishes, all of the force in the cord direction is carried by the cord. The stress perpendicular to the cords, as well as the shear stress, is assumed to be carried by the matrix. The matrix stress distribution is then transformed back to the original principal directions so that it can be compared with the distribution obtained directly from the net analysis. In addition, the cord loads from this analysis can be compared with those of the net theory. Again, it is assumed that alternate plies carry the same loads, that the laminate is composed of an even number of plies, and that each ply is geometrically and materially the same except for the cord angle. As in the net, the continuum is presumed to be two dimensional only.

Figure 5 shows a general two-dimensional stress state applied to an element of a symmetric angle-ply structure. In this sketch, y and x again represent the principal directions, and S_y, S_x, and S_{yx} are the applied stresses. This element will be analyzed in detail below, and the results will be readily adaptable to any structure with an even number of plies alternately laid up such that the cords make an angle of $\pm\,\alpha$ with the y-axis.

Applying the generalized Hooke's Law to each of the plies, the strain-stress relations are found to be as follows:

Ply 1 $(+\alpha)$

$$\begin{aligned} \epsilon_y &= a_{11}\sigma_y + a_{12}\sigma_x + a_{13}\sigma_{yx} \\ \epsilon_x &= a_{21}\sigma_y + a_{22}\sigma_x + a_{23}\sigma_{yx} \\ \epsilon_{yx} &= a_{31}\sigma_y + a_{32}\sigma_x + a_{33}\sigma_{yx} \end{aligned} \tag{25}$$

Ply 2 $(-\alpha)$

$$\begin{aligned} \epsilon_y &= a_{11}\sigma'_y + a_{12}\sigma'_x - a_{13}\sigma'_{yx} \\ \epsilon_x &= a_{21}\sigma'_y + a_{22}\sigma'_x - a_{23}\sigma'_{yx} \\ \epsilon_{yx} &= -a_{31}\sigma'_y - a_{32}\sigma'_x + a_{33}\sigma'_{yx} \end{aligned} \tag{26}$$

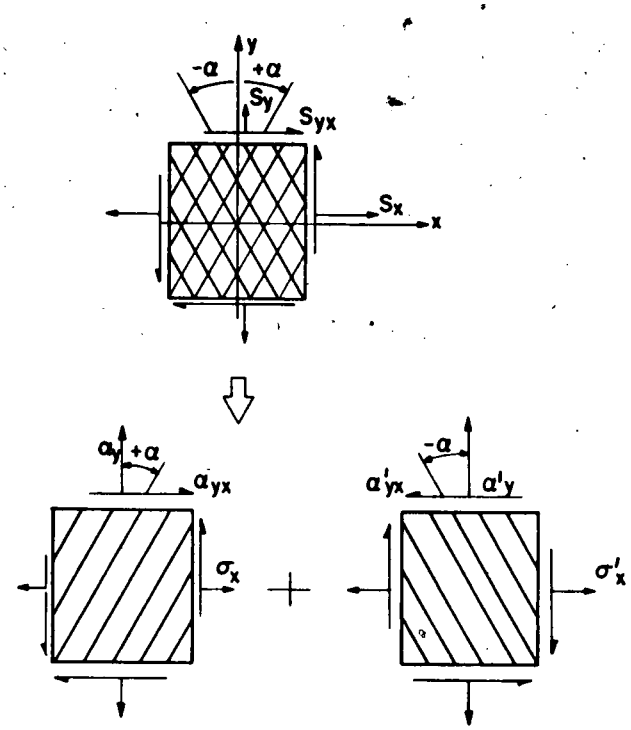

Fig. 5. Loaded element of symmetric laminate.

Here, the σ and σ' are the individual ply stresses. The ϵ represent the extensional and shearing strains while the a_{ij} are the elastic constants associated with the individual plies. The ϵ are the same in each ply, since the assembly deforms as a bonded unit. The a_{ij} have been studied in some detail by Clark [3, 4], and it has been found that each a_{ij} can be determined by knowing only basic geometric, elastic and constructional properties of the individual ply.

In addition to the strain–stress relations, force equilibrium requires that

$$\begin{aligned} 2S_y &= \sigma_y + \sigma'_y \\ 2S_x &= \sigma_x + \sigma'_x \\ 2S_{yx} &= \sigma_{yx} + \sigma'_{yx} \end{aligned} \tag{27}$$

Equations 25, 26, and 27 represent a system of nine equations and nine unknowns ϵ_y, ϵ_x, ϵ_{yx}, σ_y, σ_x, σ_{yx}, σ'_y, σ'_x, σ'_{yx}. Solving these equations simultaneously gives the following expressions for the stresses

$$\begin{aligned} \sigma_y &= \sigma'_y = S_y - \left(\frac{a_{22}a_{13} - a_{23}a_{12}}{a_{11}a_{22} - a^2_{12}}\right) S_{yx} \\ \sigma_x &= \sigma'_x = S_x - \left(\frac{a_{11}a_{23} - a_{12}a_{13}}{a_{11}a_{22} - a^2_{12}}\right) S_{yx} \\ \sigma_{yx} &= -\sigma'_{yx} = -\frac{a_{21}}{a_{23}}\sigma_y - \frac{a_{22}}{a_{23}}\sigma_x + S_{yx} \end{aligned} \tag{28}$$

The first step in determining the fraction of the applied load carried by the cords and the fraction by the matrix is to transform the stress states of each of the plies in Figure 5 into directions along the cords and perpendicular to them, as shown in Figure 6. The transformed stresses can be obtained from the well-known equations of a Mohr's circle analysis.

For ply 1:

$$\sigma_c=\left(\frac{\sigma_y+\sigma_x}{2}\right)+\left(\frac{\sigma_y-\sigma_x}{2}\right)\cos 2\alpha+\sigma_{yx}\sin 2\alpha$$

$$\sigma_1=\left(\frac{\sigma_y+\sigma_x}{2}\right)-\left(\frac{\sigma_y-\sigma_x}{2}\right)\cos 2\alpha-\sigma_{yx}\sin 2\alpha \quad (29)$$

$$\tau=-\left(\frac{\sigma_y-\sigma_x}{2}\right)\sin 2\alpha+\sigma_{yx}\cos 2\alpha$$

For ply 2:

$$\sigma'_c=\left(\frac{\sigma'_y+\sigma'_x}{2}\right)+\left(\frac{\sigma'_y-\sigma'_x}{2}\right)\cos 2\alpha-\sigma'_{yx}\sin 2\alpha$$

$$\sigma'_1=\left(\frac{\sigma'_y+\sigma'_x}{2}\right)-\left(\frac{\sigma'_y-\sigma'_x}{2}\right)\cos 2\alpha+\sigma'_{yx}\sin 2\alpha \quad (30)$$

$$\tau'=\left(\frac{\sigma_y'-\sigma'_x}{2}\right)\sin 2\alpha+\sigma'_{yx}\cos 2\alpha$$

Rewriting Equations 29 and 30 in terms of Equation 28 gives the transformed stresses in terms of known quantities.

$$\sigma_c=[\cos^2\alpha-2\sin\alpha\cos\alpha\cdot c_3]\cdot S_y+[\sin^2\alpha-2\sin\alpha\cos\alpha\cdot c_4]\cdot S_x+[-\sin^2\alpha\cdot c_1-\cos^2\alpha\cdot c_2+2\sin\alpha\cos\alpha]\cdot S_{yx} \quad (31)$$

where:

$$c_1=\left(\frac{a_{11}a_{23}-a_{12}a_{13}}{a_{11}a_{22}-a^2_{12}}\right)$$

$$c_2=\left(\frac{a_{22}a_{13}-a_{23}a_{12}}{a_{11}a_{22}-a^2_{12}}\right)$$

$$c_3=\frac{a_{31}}{a_{33}},\quad c_4=\frac{a_{32}}{a_{33}}$$

$$\sigma_1=[\sin^2\alpha+2\sin\alpha\cos\alpha\cdot c_3]\cdot S_y+[\cos^2\alpha+2\sin\alpha\cos\alpha\cdot c_4]\cdot S_x+[-\sin^2\alpha\cdot c_2-\cos^2\alpha\cdot c_1-2\sin\alpha\cos\alpha]\cdot S_{yx} \quad (32)$$

$$\tau=[-\sin\alpha\cos\alpha-(\cos^2\alpha-\sin^2\alpha)\cdot c_3]\cdot S_y+[\sin\alpha\cos\alpha-(\cos^2\alpha-\sin^2\alpha)\cdot c_4]\cdot S_x+[\sin\alpha\cos\alpha\cdot(c_2-c_1)+\cos^2\alpha-\sin^2\alpha]\cdot S_{yx} \quad (33)$$

$$\sigma'_c=[\cos^2\alpha-2\sin\alpha\cos\alpha\cdot c_3]\cdot S_y+[\sin^2\alpha-2\sin\alpha\cos\alpha\cdot c_4]\cdot S_x+[\cos^2\alpha\cdot c_2+\sin^2\alpha\cdot c_1-2\sin\alpha\cos\alpha]\cdot S_{yx} \quad (34)$$

$$\sigma'_1=[\sin^2\alpha+2\sin\alpha\cos\alpha\cdot c_3]\cdot S_y+[\cos^2\alpha+2\sin\alpha\cos\alpha\cdot c_4]\cdot S_x+[\sin^2\alpha\cdot c_2+\cos^2\alpha\cdot c_1+2\sin\alpha\cos\alpha]\cdot S_{yx} \quad (35)$$

$$\tau'=[\sin\alpha\cos\alpha+(\cos^2\alpha-\sin^2\alpha)\cdot c_3]\cdot S_y+[-\sin\alpha\cos\alpha+(\cos^2\alpha-\sin^2\alpha)\cdot c_4]\cdot S_x+[\sin\alpha\cos\alpha\cdot(c_2-c_1)+\cos^2\alpha-\sin^2\alpha]\cdot S_{yx} \quad (36)$$

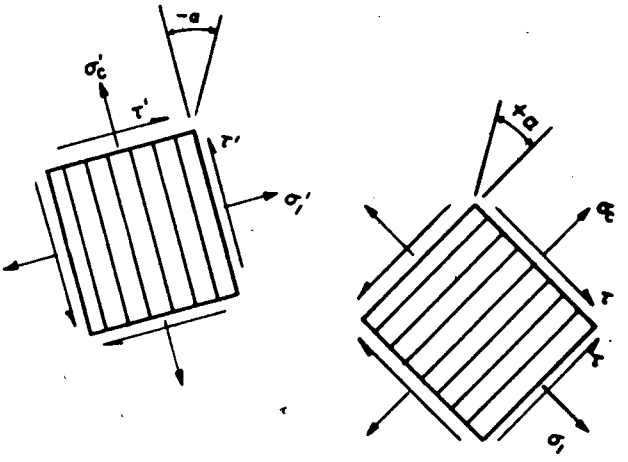

Fig. 6. Transformed stress distribution.

In order to determine the fraction of this stress distribution carried by the cords and the fraction carried by the matrix, it is useful to recall that this continuum analysis is to be compared with the net analysis in which the cords are assumed to be inextensible. Thus, to a first approximation, the strain in the cord direction is assumed zero. Therefore, for ply 1, the strain in the cord direction for the matrix is

$$\epsilon_c=\frac{R}{E}-\frac{\mu\sigma_1}{E}$$

where it is assumed that all of σ_1 and τ are carried by the matrix. R is the matrix stress in the cord direction. However, since $\epsilon_c \simeq 0$, $R \simeq \mu\sigma_1$. Thus, in order for the strain in the cord direction to be approximately zero, there must be an additional stress $\mu\sigma_1$ acting in the cord direction of the matrix. This implies that all of σ_c is not carried by the cord. Some of σ_c, an amount equal to $\mu\sigma_1$, is carried by the matrix. Thus, the total stress carried by the cord is $(\sigma_c - \mu\sigma_1)$. This results in a cord load for ply 1 of

$$T_0 = (\sigma_c - \mu\sigma_1)\cdot h/n_c$$

and for ply 2, (37)

$$Q_0 = (\sigma'_c - \mu\sigma'_1)\cdot h/n_c$$

These cord loads may be compared with those of the net analysis (Eqs. 12).

Assuming that the load carried by the cords is as given above, the stress distribution of Figure 6 can be re-examined, based on the distribution shown in Figure 7. However, to compare the matrix stresses of Figure 7 with those of the net analysis (Eqs. 6 and 7), it is necessary to transform them back to the original principal directions and recombine them into a single stress distribution. Figure 8 illustrates this transformation and recombination.

Again, using a Mohr's circle analysis;

$$\begin{aligned}
(\sigma_y)_M &= \sigma_1[c_5 + c_6\cdot\cos2\alpha] - \tau\sin2\alpha \\
(\sigma_x)_M &= \sigma_1[c_5 - c_6\cdot\cos2\alpha] + \tau\sin2\alpha \\
(\tau)_M &= \sigma_1\cdot c_6\cdot\sin2\alpha + \tau\cos2\alpha \\
(\sigma'_y)_M &= \sigma'_1[c_5 + c_6\cdot\cos2\alpha] + \tau'\sin2\alpha \\
(\sigma'_x)_M &= \sigma'_1[c_5 - c_6\cdot\cos2\alpha] - \tau'\sin2\alpha \\
(\tau')_M &= -\sigma'_1[c_6\cdot\sin2\alpha] + \tau'\cos2\alpha
\end{aligned} \tag{38}$$

where the subscript M refers to matrix stresses in the individual plies, and where

$$c_5 = \frac{\mu+1}{2}, \quad c_6 = \frac{\mu-1}{2}$$

The combined stresses are

$$\begin{aligned}
2t_y &= (\sigma_1+\sigma'_1)[c_5+c_6\cdot\cos2\alpha] - (\tau-\tau')\sin2\alpha \\
2t_x &= (\sigma_1+\sigma'_1)[c_5-c_6\cdot\cos2\alpha] + (\tau-\tau')\sin2\alpha \\
2t_\tau &= (\sigma_1-\sigma'_1)\cdot c_6\cdot\sin2\alpha + (\tau+\tau')\cos2\alpha
\end{aligned} \tag{39}$$

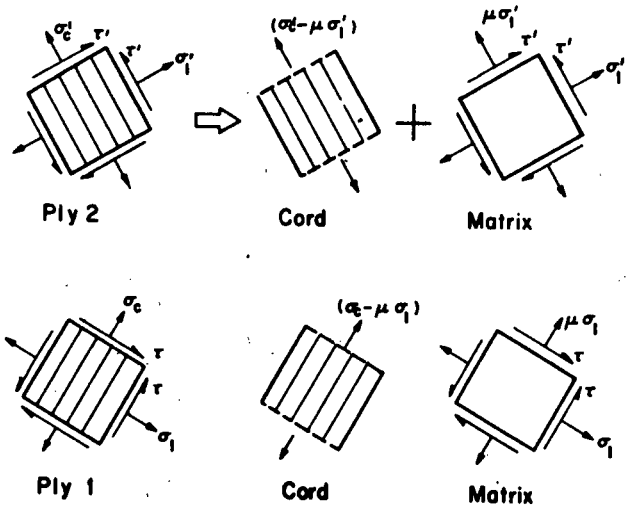

Fig. 7. Distribution of stresses carried by cord and matrix.

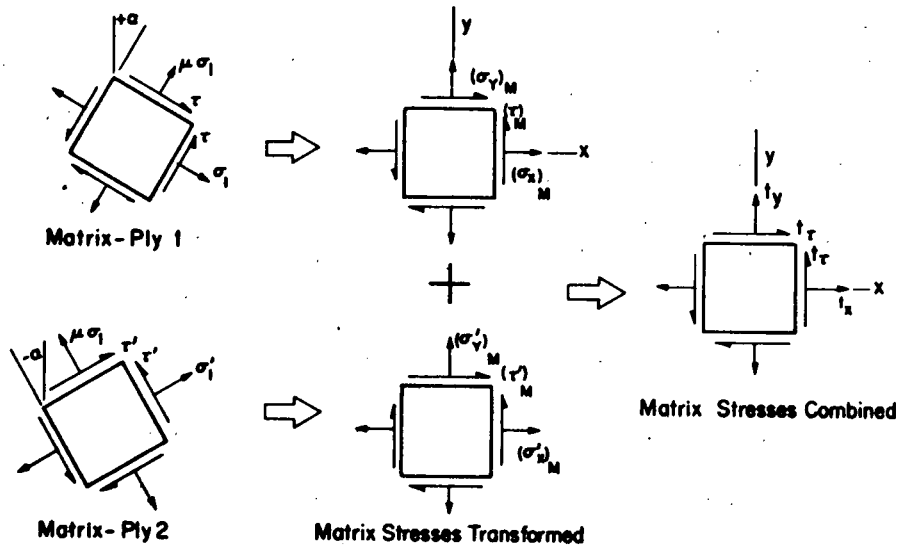

Fig. 8. Matrix stresses combined in principal directions.

The stresses in Equations 39 now represent the stress distribution in the matrix, when referred to the original principal directions of the composite structure. Thus, a direct comparison can be made between the net and continuum analyses by comparing the results obtained from Equations 39 with those obtained from Equations 6 and 7. An additional comparison can be made by comparing the cord loads obtained from Equations 12 and 37. A detailed study of these comparisons is made below.

Analytical and Numerical Comparisons

The two theories previously outlined are quite different in their philosophy. Continuum theory treats the net and matrix in its original geometry, but, in general, allows the cord to be extensible.[1] Net theory, on the other hand, considers the cord inextensible, but allows for changes in the cord angle due to deformation of the structure. Each

[1] For purposes of calculating cord loads in this paper, the cord is considered essentially inextensible compared with the matrix.

theory represents one portion of the real physical situation and, from a purely abstract point of view, it is not possible to say that one is more accurate than another. A better theory would be one incorporating the features of both approaches. For the present, it would be useful to simply compare the two theories quantitatively.

Two methods exist for comparison of the net and continuum analysis theories. In the first, the form of each result may be examined to ascertain the possibility of expressing their relative values in some analytical fashion directly. This would be most desirable, if it could be accomplished. A less attractive possibility would be to choose selected representative stress states and to evaluate the results from each of the two theories for these stress states. Both methods will be considered here.

Let us consider first the possibility of analytical evaluation of the two approaches. The results of the continuum approach are rather complicated algebraically. However, they may be substantially simplified by noting that the elastic coefficients a_{ij} take on a greatly reduced form when one uses the physical fact that the extension modulus of a single ply of material with parallel inextensible reinforcing cords is indefinitely large in the cord direction compared to the extension modulus perpendicular to the cords. Although the algebra is lengthy, it may be shown that such an assumption leads to a simple form for two of the constants previously defined, i.e.,

$$c_1 \simeq \tan\alpha \quad c_2 \simeq -\cot\alpha$$

Using these in Equations 32, 33, 34, and 35 gives

$$\sigma_c = [\cos^2\alpha - 2\sin\alpha\cos\alpha \cdot c_3]\cdot S_y + [\sin^2\alpha - 2\sin\alpha\cos\alpha\cdot c_4]\,S_x + \left[\frac{\sin^2\alpha}{\cos\alpha} + \frac{\cos^2\alpha}{\sin\alpha} + 2\sin\alpha\cos\alpha\right] S_{yx} \tag{40}$$

$$\sigma_1 = \sigma'_1 = [\sin^2\alpha + 2\sin\alpha\cos\alpha\cdot c_3]\,S_y + [\cos^2\alpha + 2\sin\alpha\cos\alpha\cdot c_4]\,S_x \tag{41}$$

$$\tau = -\tau' = [-\sin\alpha\cos\alpha - (\cos^2\alpha - \sin^2\alpha)\cdot c_3]\cdot S_y + [\sin\alpha\cos\alpha - (\cos^2\alpha - \sin^2\alpha)\cdot c_4]\cdot S_x \tag{42}$$

$$\sigma'_c = [\cos^2\alpha - 2\sin\alpha\cos\alpha\cdot c_3]\,S_y + [\sin^2\alpha - 2\sin\alpha\cos\alpha\cdot c_4]\,S_x - \left[\frac{\cos^2\alpha}{\sin\alpha} + \frac{\sin^2\alpha}{\cos\alpha} + 2\sin\alpha\cos\alpha\right] S_{yx} \tag{43}$$

If Equations 41 and 42 are used with Equation 39, one may obtain the following expressions for the stress carried by the matrix

$$\begin{aligned} t_y &= \sigma_1[c_5 + c_6\cos 2\alpha] - \tau\sin 2\alpha \\ t_x &= \sigma_1[c_5 - c_6\cos 2\alpha] + \tau\sin 2\alpha \\ t_\tau &= 0 \end{aligned} \tag{44}$$

Thus, the simplification associated with neglecting the small ratio of modulus perpendicular to cords/to modulus parallel to cords in a single sheet is sufficient to cause the continuum theory to predict zero shear stress carried by the matrix. This coincides exactly with the results from net theory, and in this respect the two theories are identical.

As a further check, let us consider the special case where the cord angle $\alpha = 45°$, $S_{xy} = 0$ and $S = S_x = S_y$. Net analysis, from Equation 24, predicts no angle change; hence, no deformation, so that the matrix stresses t_x and t_y are zero. The resulting cord loads are given by Equation 12 in the form of

$$Q_0 = T_0 = \frac{2Sh}{n_c}$$

It may readily be shown that, for $\alpha = 45°$,

$$c_3 = c_4 = -\tfrac{1}{2}$$

so that the continuum theory of Equations 41 and 42 gives

$$\sigma_1 = \sigma'_1 = 0$$
$$\tau = \tau' = 0$$

This means that the matrix stresses are zero, from reference to Equation 44, which again is in agreement with the net theory, as is the cord load. This latter quantity may be evaluated for this case from Equations 40 and 43 which give

$$\sigma_c = \sigma'_c = 2S$$

Using Equations 37 then allows cord loads to be derived

$$T_0 = Q_0 = \frac{2Sh}{n_c}$$

as was obtained above for the net.

Another method of comparison of the two theories is by direct numerical evaluation. Fortunately, it is possible to do this in a dimensionless form, but it is necessary to restrict attention to a few simple but illustrative cases. First, continuum theory is made much easier computationally by assuming that the modulus of a single ply in the cord direction is indefinitely large compared with the modulus in

other directions. Second, we restrict attention to two simple stress states, one of pure tension and one of pure shear.

Taking first the case of pure tension, it is possible to compare the angle changes predicted by the small-displacement net theory (Equ. 10) with those given by the finite deformation net theory (Equ. 24). The latter should be more exact and would in general be preferred for computation. Using several different values of a dimensionless applied tension S_y/E and a range of initial cord angles, the final cord angles may be computed for both forms of net theory and are presented in Table I. Here, it is seen that the final cord angles are nearly the same for both theories if the applied stresses are small ($S_y/E = 0.01$, $S_y/E = 0.05$), while for larger stresses, the differences between small strain and finite deformation theory become greater. Generally speaking, the greatest differences seem to appear at large stresses and large cord angles, where the finite deformation net theory predicts somewhat greater angle change.

TABLE I. Final Cord Angles for Different Initial Cord Angles, Stress Levels, and Net Theories

Initial cord angle deg	Final cord angle—Net theory							
	$S_y/E = 0.01$		$S_y/E = 0.05$		$S_y/E = 0.10$		$S_y/E = 0.30$	
	Small strain	Finite def.	Small strain	Finite def.	Small strain	Finite def.	Small strain	Finite def.
10	9.997	9.997	9.988	9.988	9.975	9.975	9.928	9.929
20	19.976	19.976	19.884	19.885	19.772	19.775	19.350	19.376
30	29.893	29.895	29.492	29.501	29.029	29.060	27.486	27.672
40	39.684	39.687	38,538	38.567	37.310	37.413	33.766	34.297
50	49.543	49.543	47.775	47.730	45.702	45.604	39.254	39.665
60	59.678	59.673	58.371	58.272	56.674	56.253	49.109	46.261
70	69.821	69.816	69.105	69.051	68.196	67.950	64.319	61.239
80	79.919	79.919	79.606	79.584	79.212	79.114	77.618	76.486

Cords loads may be predicted by either net or continuum theory for a state of simple tension S_y as the only nonzero stress component. This may be done by continuum theory methods by letting the modulus E_x in the cord direction approach infinity, and the associated Poisson's ratio approach zero. This simplifies the expressions for the elastic constants in the plane orthotropic case so that

$$a_{13} = -2\sin^3\alpha\cos\alpha/E_y - \cos\alpha\sin\alpha(\cos^2\alpha - \sin^2\alpha)/G_{xy}$$
$$a_{33} = 4\sin^2\alpha\cos^2\alpha/E_y + (\cos^2\alpha - \sin^2\alpha)^2/G_{xy}$$

It may be shown, by considering the cords to be inextensible, that the ratio of shear modulus G_{xy} to modulus perpendicular to cords E_y is given by

$$G_{xy}/E_y = \tfrac{1}{4}$$

With these relations,

$$c_3 = -\sin\alpha\cos\alpha(\cos^2\alpha - 0.5\sin^2\alpha)/(\cos^4\alpha - \sin^2\alpha\cos^2\alpha + \sin^4\alpha)$$

and

$$\sigma_c = S_y(\cos^2\alpha - 2c_3\sin\alpha\cos\alpha)$$
$$\sigma_1 = \sigma'_1 = S_y(\sin^2\alpha + 2c_3\sin\alpha\cos\alpha)$$
$$\tau = -\tau' = -S_y[\sin\alpha\cos\alpha + c_3(\cos^2\alpha - \sin^2\alpha)]$$

This may be used to obtain

$$T_0 \cdot n_c/h = \sigma_c - 0.5\sigma_1$$
$$t_y = \sigma_1(0.75 - 0.25\cos 2\alpha) - \tau\sin 2\alpha$$
$$t_x = \sigma_1(0.75 + 0.25\cos 2\alpha) + \tau\sin 2\alpha$$
$$t_\tau = 0$$

For finite-deformation net theory (Equ. 24) must first be used to obtain a final deformed cord angle. Then the following quantities can be derived

$$t_x = \frac{E}{3}\left(\lambda_x - \frac{1}{\lambda^3_x\lambda^2_y}\right)$$

$$t_y = \frac{E}{3}\left(\lambda_y - \frac{1}{\lambda^2_x\lambda^3_y}\right)$$

$$N/n_p = S_y \cdot h - t_y \cdot H$$
$$T_0 = Q_0 = N/n_p n_c \cos^2\alpha$$

For these calculations, we assume that the cord diameter is negligible, so that

$$H \simeq h$$

This conforms to the assumption used in the continuum theory, where the influence of cord area is neglected,

Cord loads are calculated on this basis for a range of cord angles, using continuum theory as one form and two different stress levels in net theory as the other form. These results are given in Figure 9, where it is seen that very little difference exists between the two forms over most of the range of cord angles. Only at angles in excess of about 65° do the net theory cord loads for small stresses differ substantially from the continuum theory and the net theory for $S_y/E = 0.1$. The latter two are almost identical over the entire range of cord angles.

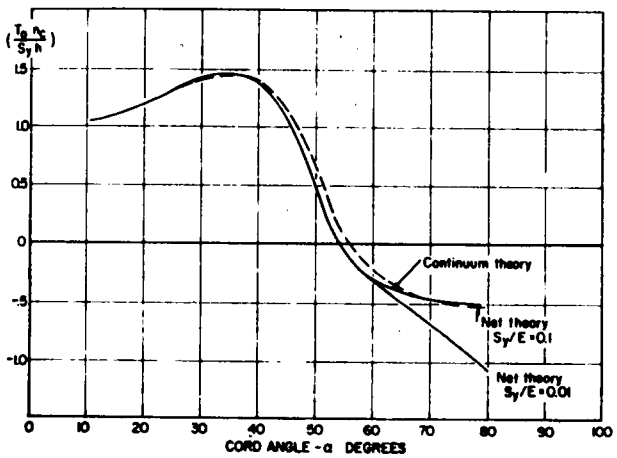

Fig. 9. Dimensionless cord load caused by pure tension vs cord angle.

Similar results are obtained for the matrix stresses t_y, in the applied stress direction, and t_x in the direction perpendicular to the applied stresses. These are plotted in Figures 10 and 11. Again, it is seen that continuum theory and net theory for $S_y/E = 0.01$ and $S_y/E = 0.1$ are essentially identical.

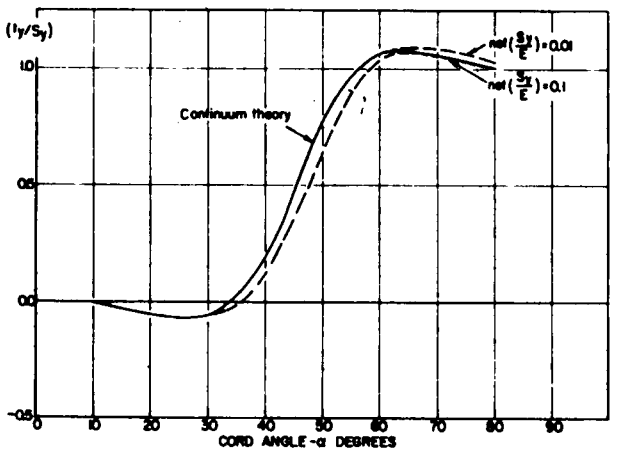

Fig. 10. Dimensionless matrix stresses due to pure tension S_y vs cord angle.

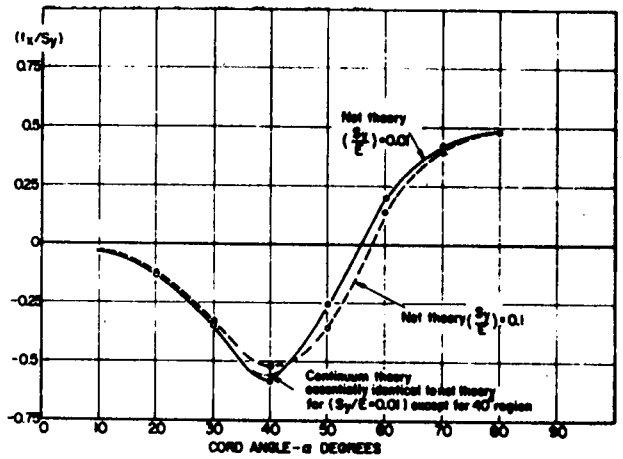

Fig. 11. Dimensionless matrix stresses due to pure tension S_y vs cord angle.

For an applied shear stress S_{xy}, with no applied normal stresses S_x and S_y, it may be shown that the finite-deformation net theory gives

$$T_0 = -Q_0 = S_{xy} \cdot h/n_c \cdot \sin\alpha \cos\alpha$$
$$t_x = t_y = 0$$

For continuum theory, one must calculate the following quantities

$$a_{11} = \sin^4\alpha/4 + \sin^2\alpha \cos^2\alpha$$
$$a_{12} = -0.75 \sin^2\alpha \cos^2\alpha$$
$$a_{22} = 0.25 \cos^4\alpha + \sin^2\alpha \cos^2\alpha$$
$$a_{23} = -\sin\alpha \cos^2\alpha/2 + \sin\alpha \cos\alpha(\cos^2\alpha - \sin^2\alpha)$$
$$a_{13} = -\sin^2\alpha \cos\alpha/2 - \sin\alpha \cos\alpha(\cos^2\alpha - \sin^2\alpha)$$
$$a_{33} = \sin^2\alpha \cos^2\alpha + (\cos^2\alpha - \sin^2\alpha)^2$$

From these, one obtains

$$c_1 = (a_{11}a_{23} - a_{12}a_{13})/(a_{11}a_{22} - a^2_{12})$$
$$c_2 = (a_{22}a_{13} - a_{23}a_{12})/(a_{11}a_{22} - a^2_{12})$$

from which

$$\sigma_c = S_{xy}(c_1 \sin^2\alpha + c_2 \cos^2\alpha - 2\sin\alpha \cos\alpha)$$

and the cord load is

$$T'_0 = \frac{\sigma_c h}{n_c}$$

Values of cord tension T_0 and T'_0 for net and continuum theories were calculated for this condition of shear stress and were found to be identical for all cord angles. They are shown in Figure 12. Values

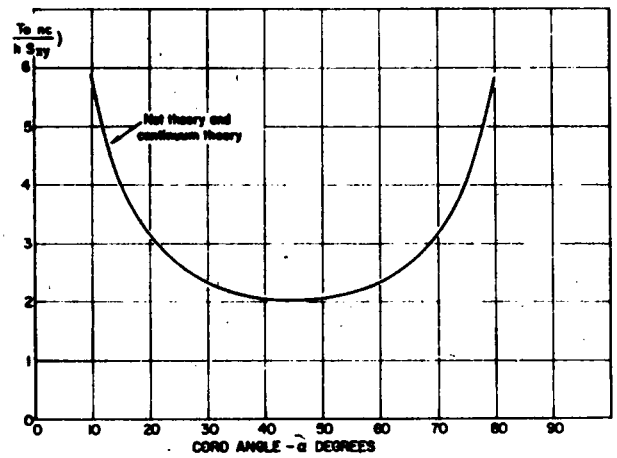

Fig. 12. Dimensionless cord load due to applied shear stress S_{xy} vs cord angle.

of shear stress carried by the matrix for continuum theory were calculated and found to be zero, as is the matrix shear stress from net theory. Thus, for shear stresses applied to a body net and continuum theory give identical results.

Literature Cited

1. Akasaka, T., *Trans. Commemoration 80th Anniversary Chuo University*, Tokyo, 1965, p. 81–114.
2. Azzi, V. D. and Tsai, S. W., Presented at SESA Annual Meeting, Cleveland, Ohio, October 1964.
3. Clark, S. K., *Textile Res. J. 33*, 295–313 (1963).
4. Clark, S. K., *Textile Res. J. 33*, 935–953 (1963).
5. Hofferberth, W. and Frank, F., *Rubber Chem. Technol.* **40** p. 271–322 (Feb. 1967).
6. Reissner, E. and Stavsky, Y., *J. Appl. Mech.* **28**, No. 402, 1961.
7. Treloar, L. R. G., "The Physics of Rubber Elasticity," Oxford-The Clarendon Press, 1949.
8. Whitney, J. M., *Expll. Mechanics* **7**, 447–448 (1967).

Manuscript received February 27, 1968.

Flexing Fatigue of Glass-Fiber Filter Cloth

R. E. Hicks and W. G. B. Mandersloot

Council for Scientific and Industrial Research, Chemical Engineering Group, Pretoria, South Africa

Abstract

A flexing endurance test, using a modification of ASTM D643-43 for paper, is suitable for the evaluation of glass-fiber filter cloth. The test can be applied to new cloths and cloths after exposure to heat, this being the major cause of deterioration of the cloth properties in practice. Superior flexing endurance, when new, is not necessarily maintained after heat exposure.

The life distribution is log-normal for the texturized-yarn weft direction and bi-modal log-normal for the continuous-filament-yarn warp direction. For the warp, a two-stage mechanism leading to failure is evident from the observed specimen elongations; for the weft, only one stage was observed.

The log of life is inversely proportional to the flexing angle, which is explained by considering the flexing angle (proportional to the length of specimen being flexed) as an equivalent of specimen length in axial-stress cycle fatigue.

Introduction

Bag filtration is one of the most effective means of fine-dust collection [8] but it results in difficulties when applied to the high-temperature (>300°F) filtration which is desirable in order to minimize the expense and corrosion dangers resulting from the cooling of hot gases [20]. A material is required that is temperature-resistant and capable of withstanding, at elevated temperatures, the mechanical wear experienced during the removal of the filter cake. The latter is effected by reversing the gas flow which causes partial collapse of the filter bag tubes, with simultaneous vibration of either the bag or, using sonic energy, the gas. In some cases, e.g., carbon black filtration, the frequency of this cleaning cycle is high due to the high dust load and the high